

Multiple-layered structure of obelisk-shaped crystalline nano-ZnO prepared by sol–gel route

Saeideh Jurablu¹ · Majid Farahmandjou¹ · Tahereh Pormirjaafari Firoozabadi¹

Received: 31 January 2015 / Accepted: 29 July 2015 / Published online: 21 August 2015
© The Author(s) 2015. This article is published with open access at Springerlink.com

Abstract Zinc oxide nanopowders were synthesized by the simple sol–gel method from an ethanol solution of zinc nitrate hexahydrate. Structural and surface morphological investigations were carried out using X-ray diffraction (XRD), high-resolution transmission electron microscopy (HRTEM), scanning electron microscopy, Fourier transform infrared spectroscopy (FTIR) and ultraviolet–visible (UV–Vis) spectrophotometry analyses. XRD pattern showed that the zinc oxide nanoparticles exhibited hexagonal wurtzite structure. A multiple-layered structure of obelisk-shaped ZnO nanoparticles was achieved after calcinations. The average particle size of ZnO was around 20 nm as estimated by direct HRTEM observation. The size of sphere-like shaped ZnO nanoparticles was measured in the range of 20–80 nm and the size of pyramid-like shaped annealed samples was achieved in the range of 40–100 nm with less agglomeration. The energy dispersive spectroscopy spectrum showed peaks of zinc and oxygen. The sharp peaks in FTIR spectrum determined the Zn–O stretching and absorbance peak of UV–Vis spectrum showed the wide bandgap energy of 3.35 eV.

Keywords ZnO nanoparticles · Obelisk-shaped · Synthesis · Sol–gel

Introduction

ZnO has received lot of attention as a nanostructured material because of its unique properties rendering it suitable for various applications. One-dimensional nanostructures exhibit interesting electronic and optical properties due to their low dimensionality leading to quantum confinement effects. The novel properties of nanoscale zinc oxide particles have found applications in a variety of applications such as luminescence [1–3], varistors [4, 5], solar cells [6], gas sensors [7, 8]. Many of the synthetic approaches such as sol–gel method [13], co-precipitation [12], hydrothermal method [14], microwave synthesis [9–11], and thermal evaporation method [15] have been used for the preparation of ZnO powders. Amongst the different methods of synthesis of ZnO nanostructures, the sol–gel method is attractive for its simplicity and environment-friendly conditions. Sol–gel preparation of solid catalysts has been reported by many research groups [16–20]. Using this method, the crystal grain can develop completely and the particle size is uniform. The soft-chemistry routes especially sol–gel procedures offer unique advantages such as the possibility of obtaining metastable materials, achieving superior purity and compositional homogeneity of the products at moderate temperatures with simple laboratory equipment [21]. Semiconductor photo-catalysts offer huge potential for elimination of toxic chemicals [22]. ZnO, with band gap = 3.37 eV, has become promising in the past few years because of its distinctive optoelectronic, catalytic, and photochemical properties [24, 25]. It crystallizes in a hexagonal wurtzite structure (zincite). The ZnO-mediated photocatalytic process has been successfully used to degrade organic pollutants [23, 26]. The aim of this study was to synthesize zinc oxide of low dimension and investigate the morphological properties and surfactant

✉ Majid Farahmandjou
farahmandjou@iauvaramin.ac.ir

¹ Department of Physics, Varamin Pishva Branch, Islamic Azad University, Varamin, Iran

Fig. 1 XRD pattern of ZnO nanoparticles: **a** as prepared, **b** annealed sample

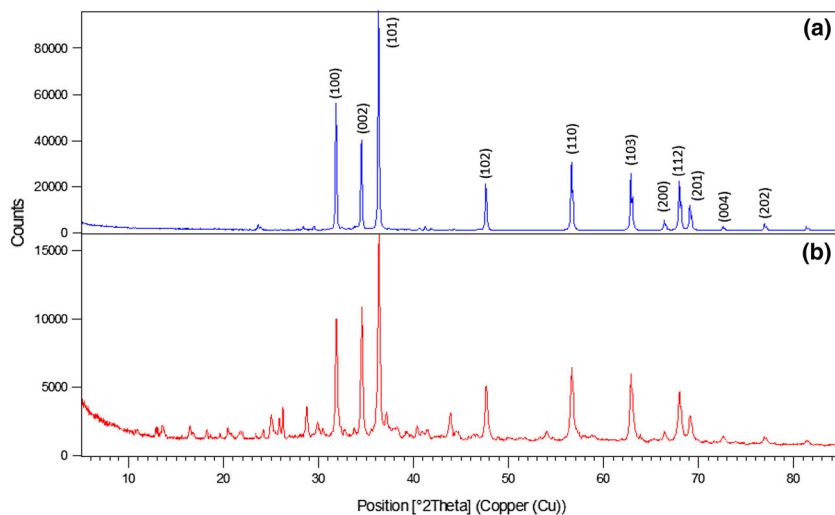


Fig. 2 SEM images of the **a** as-prepared, **b** annealed ZnO nanoparticles at 500 °C

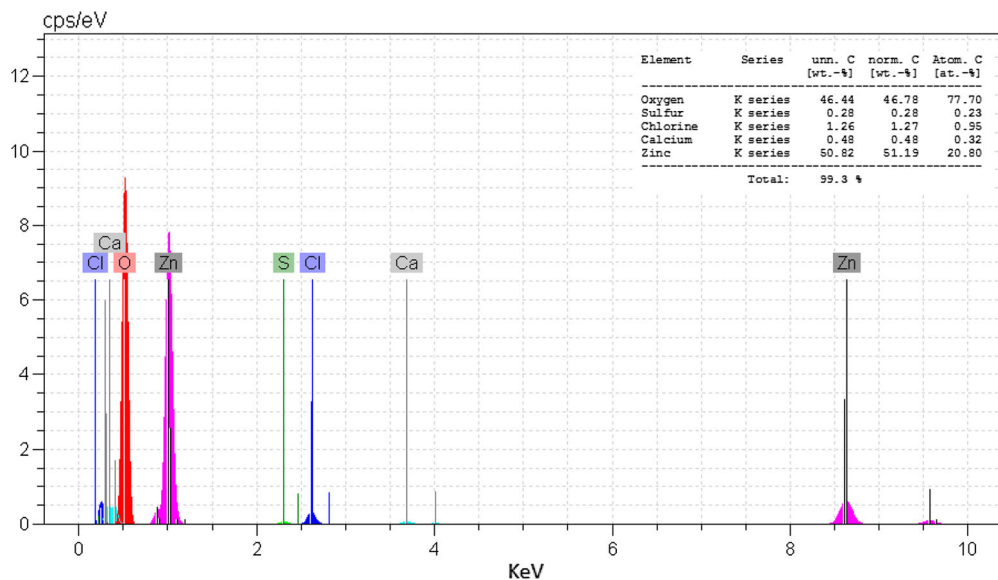
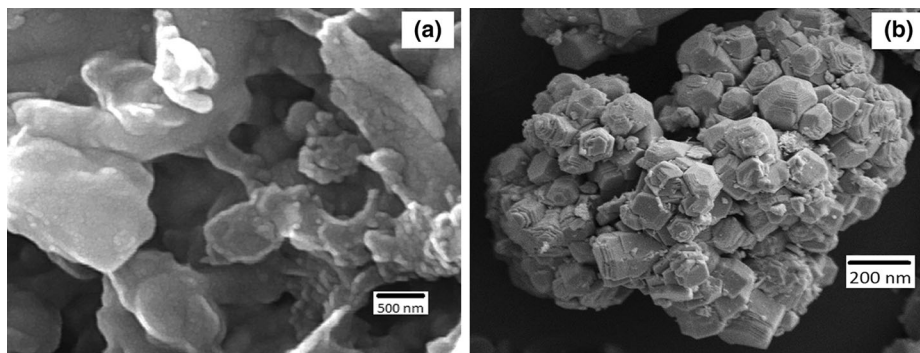


Fig. 3 EDS spectra of the as-synthesized ZnO prepared by wet synthesis

effect on the particle size. This method has features, which are of considerable interest due to its low cost, easy preparation and industrial viability. The novelty of this method is that the samples were not purified and centrifuged in the fabrication stage because of oxidation. In many synthesis methods, the researchers purified samples to have uniform particles which oxidize ZnO nanoparticles by purification and centrifugation process [2, 8, 10–15]. Synthesis of ZnO nanoparticles by sol–gel technique is reported by $\text{Zn}(\text{NO}_3)_2 \cdot 6\text{H}_2\text{O}$ precursor and calcined at 500 °C. The structural and morphological properties of ZnO have been studied by X-ray diffractometry (XRD), Fourier transform infrared spectroscopy (FTIR), ultraviolet–visible spectrophotometry (UV–Vis), spectroscopy, high-resolution transmission electron microscopy and scanning electron microscopy (SEM) analyses.

Experimental details

ZnO nanoparticles were synthesized by a new simple sol–gel approach in the following manner: In the first 30 g, $\text{ZnSO}_4 \cdot 7\text{H}_2\text{O}$ was dissolved in 150 mL deionized water and then 14 mL ethanol (99.7 %) was added to the solution. The mixed solution was stirred with a magnetic stirrer at 80 °C for 3 h to obtain the gel. The obtained gel was dried at 220 °C for 1 h and then ground into fine particles. The temperature of the dried precursor powder was increased at the rate of 1 °C/min to attain the required temperature and then the sample was allowed to stay at 500 °C for 3 h to obtain the ZnO nanoparticles.

The morphology of the as-synthesized and annealed ZnO nanoparticles was carried out. XRD was used to identify the crystalline phase and to estimate the crystalline size. The XRD patterns were recorded with 2θ in the range 4°–85° with Cu-K α : $\lambda = 1.54 \text{ \AA}$ model X – PRt PR $_{\theta}$ MPD. The morphology was characterized by an SEM model 3200 Ky-EM and transmission electron microscope (TEM) 900 ZEISSEM. All the measurements were carried out at room temperature. The optical properties of absorption were measured by UV–Vis model 300-sp and FTIR model 510-WQF.

Results and discussion

XRD at 40 kV was used to identify crystalline phases and to estimate the crystalline sizes. Figure 1a shows the XRD morphology of the as-prepared ZnO nanoparticles and Fig. 1b shows the sample annealed at 500 °C for 3 h. In our case, all the diffraction peaks at angles (2θ) of 31.36°, 34.03°, 35.8°, 47.16°, 56.26°, 62.54°, 67.64°, 68.79°, 69.45°, 72.82° and 77.33° correspond to the reflection from

(100), (002), (101), (102), (110), (103), (200), (112), (201), (004) and (202) crystal planes of the hexagonal wurtzite zinc oxide structure. The mean size of the ordered ZnO nanoparticles has been estimated from full width at half maximum (FWHM) and Debye–Scherrer formula according to the following equation: [27]:

$$D = \frac{0.89\lambda}{B \cos \theta} \quad (1)$$

where, 0.89 is the shape factor, λ is the X-ray wavelength, B is the line broadening at half the maximum intensity (FWHM) in radians, and θ is the Bragg angle. The mean size of as-prepared ZnO nanoparticles was in the range 20–50 nm from this Debye–Scherrer equation.

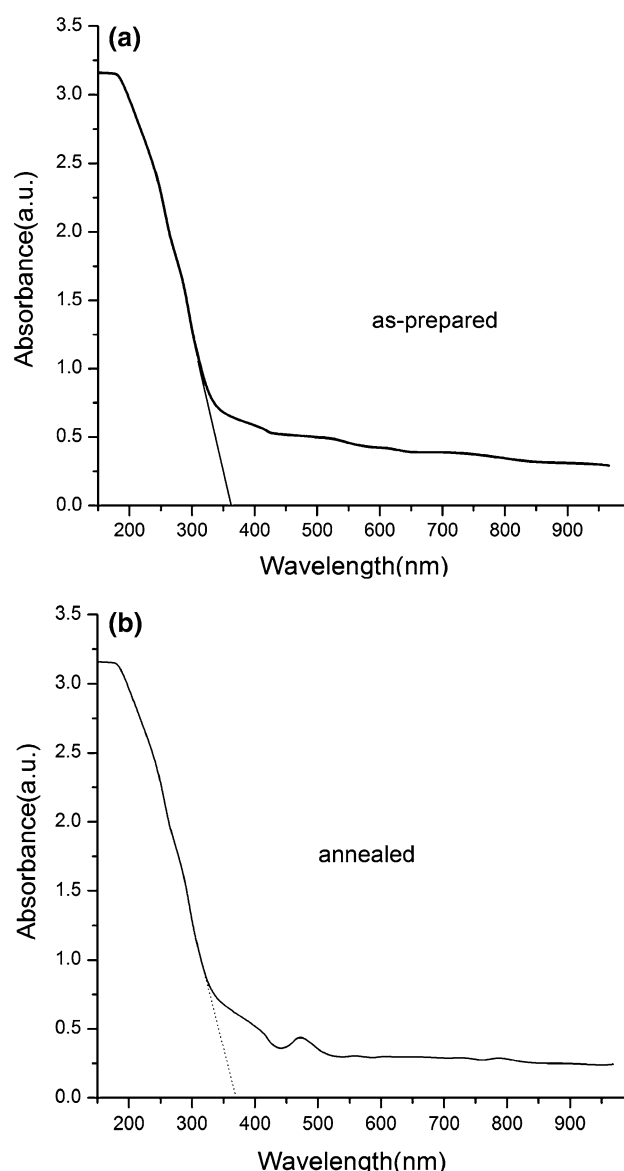


Fig. 4 UV–Vis absorption spectra of ZnO: **a** as-prepared, **b** annealed sample

SEM analysis was used for the morphological study of ZnO nanoparticles. These analyses show that the multiple layered structure of obelisk-shaped ZnO nanoparticles are formed by increasing annealing temperature [28]. With increasing temperature the morphology of the particles changes to the pyramid shape and nanopowders were less agglomerated. Figure 2a shows the SEM image of the as-prepared ZnO nanoparticles prepared by sol–gel method. In this figure, the particles were prepared with formation of clusters. Figure 2b shows the SEM image of the ZnO nanoparticles annealed at 500 °C for 3 h. It can be seen that the multiple layered of obelisk-shaped ZnO nanoparticles were less agglomerated.

Energy dispersive spectroscopy analysis of the ZnO samples is shown in Fig. 3. It confirms the existence of Zn and O with weight percent. EDS was used to analyze the chemical composition of a material under SEM. EDS measurement shows peaks of zinc and oxygen and indicates a few of impurities in prepared samples.

UV–visible absorption spectral study was done to understanding of the optical band gap of the material. Absorption in the near-ultraviolet region arises from electronic transitions associated within the sample. UV–Vis absorption spectra of as-prepared and annealed ZnO nanoparticles are shown in Fig. 4. As you can see from the pictures, the strong absorption band at a low wavelength near 370 nm corresponds to the bandgap energy of 3.35 eV for the as-prepared sample, and the strong absorption band at the low wavelength near 379 nm corresponds to 3.27 eV for the annealed nanoparticles. The size of particles changes with increasing temperature and the bandgap energy decreases with increasing annealing temperature.

Figure 5 shows the FTIR spectra of the ZnO powders, which were acquired in the range of 4000–400 cm^{-1} . All

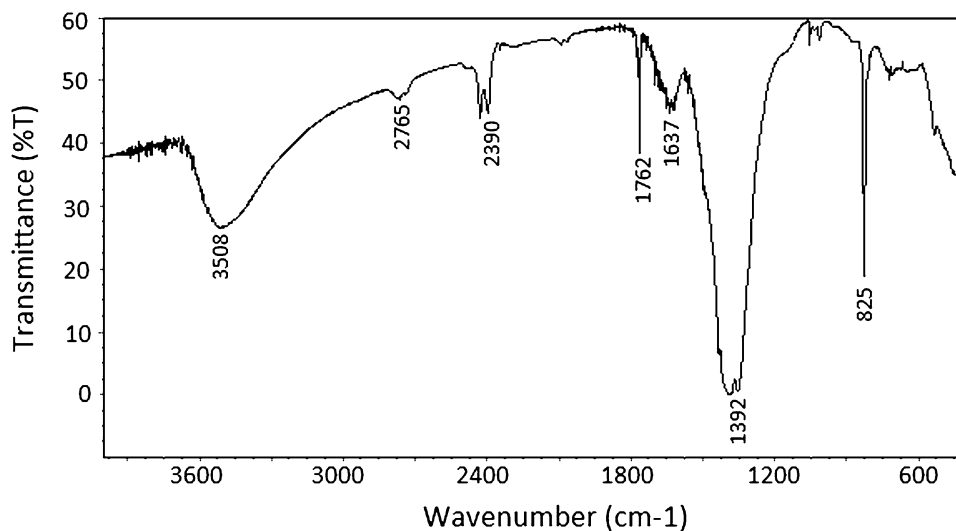
of the spectra exhibit a strong absorption peak at 3508 cm^{-1} for stretching vibration of non-chemical bond association OH groups and at 1637 cm^{-1} for H–O–H bending vibrations. The peaks at 2390 cm^{-1} are attributed to the presence of carbon dioxide. The absorption peaks around 1392 cm^{-1} are assigned to the bending vibration of C–H stretching. The peaks at 514–442 cm^{-1} are for Zn–O. The above results are in accordance with the XRD results.

The TEM analysis was carried out to confirm the actual size of the particles, their growth pattern and the distribution of the crystallites. Figure 6 shows the TEM image of spherical ZnO nanoparticles prepared by chemical sol–gel route. Figure 6a shows the as-synthesized samples with an average diameter of 20 nm. Figure 6b indicates the annealed samples with an average diameter of 80 nm. It can be seen that the size of nanoparticles increases with increasing annealing temperature. Because the increasing temperature remove the surfactants around the particles and the particles are closed to each other because of interactions.

Conclusion

A multiple-layered structure of obelisk-shaped ZnO nanoparticles was successfully synthesized by a new and simple sol–gel method using an ethanol solution of $\text{Zn}(\text{NO}_3)_2 \cdot 6\text{H}_2\text{O}$. The XRD results show that ZnO nanoparticles are hexagonal wurtzite in the size range 20–50 nm. From SEM images, it is clear that with increasing temperature, the morphology of the particles changes to the obelisk shape and the nanopowders were less agglomerated. The TEM image exhibits the as-synthesized ZnO nanoparticles prepared the by sol–gel route

Fig. 5 The Fourier transform infrared spectroscopy pattern of the zinc oxide nanoparticles



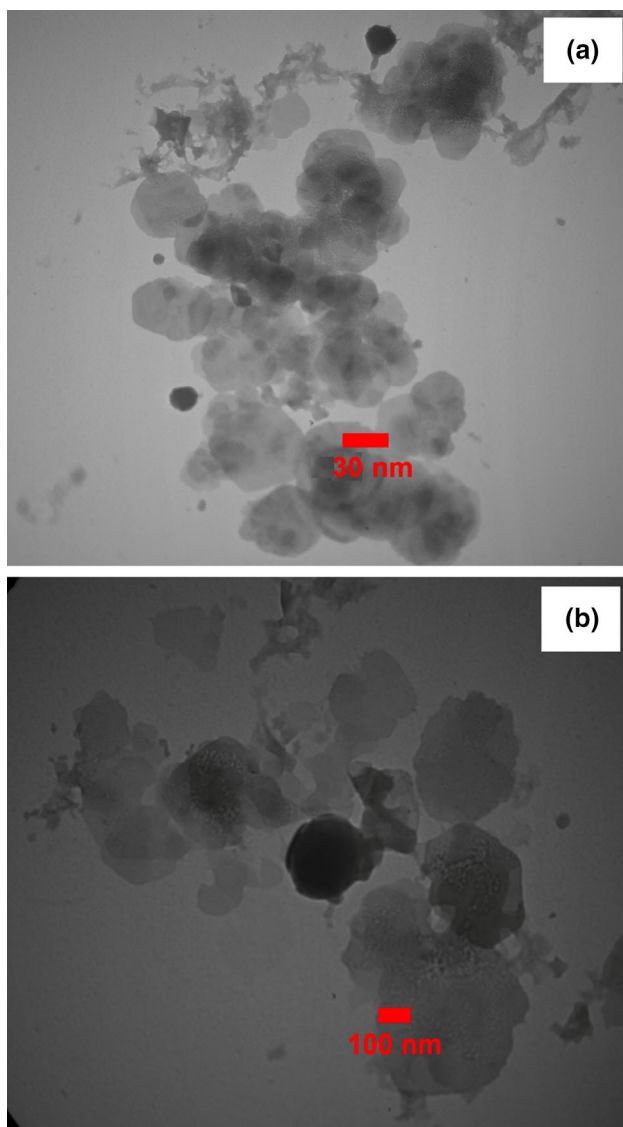


Fig. 6 TEM images of the ZnO nanoparticles: **a** as-prepared, **b** annealed samples

with average size of 20 nm. The EDS measurements showed only peaks of zinc and oxygen and indicated the absence of impurities in the prepared ZnO samples. From the FTIR data, the presence of Zn–O stretching mode of ZnO is shown. The zinc oxide nanoparticles show a strong UV–Vis absorption below 400 nm with a well-defined absorption peak at 370 nm; the direct bandgap is found to be 3.35 eV.

Acknowledgments The authors are thankful for the financial support of Varamin Pishva Branch at Islamic Azad University for analysis and the discussions on the results.

Open Access This article is distributed under the terms of the Creative Commons Attribution 4.0 International License (<http://creativecommons.org/licenses/by/4.0/>), which permits unrestricted use,

distribution, and reproduction in any medium, provided you give appropriate credit to the original author(s) and the source, provide a link to the Creative Commons license, and indicate if changes were made.

References

- van Dijken, A., Meulenkamp, E.A., Vanmaekelbergh, D., Meijerink, A.: The luminescence of nanocrystalline ZnO particles: the mechanism of the ultraviolet and visible emission. *J. Lumin.* **87–89**, 454–456 (2000)
- Guo, L., Yang, S.H., Yang, C.L., Yu, P., Wang, J.N., Ge, W.K., Wong, G.K.L.: Synthesis and characterization of poly(vinylpyrrolidone)-modified zinc oxide nanoparticles. *Chem. Mater.* **12**, 2268–2274 (2000)
- Feng, Y., Zhou, Y.X., Liu, Y.Q., Zhang, G.B., Zhang, X.Y.: Photoluminescence spectra of nano-structured ZnO thin films. *J. Lumin.* **119–120**, 233–236 (2006)
- Hingorani, S., Pillai, V., Kumar, P., Multani, M.S., Shah, D.O.: Microemulsion mediated synthesis of zinc-oxide nanoparticles for varistor studies. *Mater. Res. Bull.* **28**, 1303–1310 (1993)
- Pillai, S.C., Kelly, J.M., McCormack, D.E., O'Brien, P., Ramesh, R.: The effect of processing conditions on varistors prepared from nanocrystalline ZnO. *J. Mater. Chem.* **13**, 2586–2590 (2003)
- Beek, W.J.E., Wienk, M.M., Janssen, R.A.J.: Efficient hybrid solar cells from zinc oxide nanoparticles and a conjugated polymer. *Adv. Mater.* **16**, 1009–1013 (2004)
- Epifani, M., Diaz, R., Arbiol, J., Comini, E., Sergent, N., Pagnier, T., Siciliano, P., Taglia, G., Morante, J.R.: Nanocrystalline metal oxides from the injection of metal oxide sols in coordinating solutions: synthesis, characterization, thermal stabilization, device processing, and gas-sensing properties. *Adv. Funct. Mater.* **16**, 1488–1498 (2006)
- Tang, H.X., Yan, M., Ma, X.F., Zhang, H., Wang, M., Yang, D.R.: Gas sensing behavior of polyvinylpyrrolidone-modified ZnO nanoparticles for trimethylamine. *Sens. Actuators B* **113**, 324–328 (2006)
- Trandafilović, L.V., Božanić, D.K., Dimitrijević-Branković, S., Luyt, A.S.: Fabrication and antibacterial properties of ZnO–alginate nanocomposites. *Carbohydr. Polym. Djoković V* **88**, 263–269 (2012)
- Martins, N.C.T., Freire, C.R.S., Neto, C.P., Silvestre, A.J.D., Causio, J., Baldi, G.: Antibacterial paper based on composite coatings of nanofibrillated cellulose and ZnO. *Colloids Surf. A* **417**, 111–119 (2013)
- Jalal, R., Goharshadi, E.K., Abareshi, M., Moosavi, M., Yousefi, A., Nancarrow, P.: ZnO nanofluids: green synthesis, characterization, and antibacterial activity. *Mater. Chem. Phys.* **121**, 198–201 (2010)
- Nair, M.G., Nirmala, M., Rekha, K., Anukaliani, A.: Structural, optical, photo catalytic and antibacterial activity of ZnO and Co doped ZnO nanoparticles. *Mater. Lett.* **65**, 1797–1800 (2011)
- Talebian, N., Nilforoushan, M.R., Zargar, E.B.: Enhanced antibacterial performance of hybrid semiconductor nanomaterials: ZnO/SnO₂ nanocomposite thin films. *Appl. Surf. Sci.* **258**, 547–555 (2011)
- Phan, D.T., Chung, G.S.: Effects of defects in Ga-doped ZnO nanorods formed by a hydrothermal method on CO sensing properties. *Sens. Actuators B* **187**, 191–197 (2013)
- Li, Q., Chen, Y., Luo, L., Wang, L., Yu, Y., Zhai, L.: Photoluminescence and wetting behavior of ZnO nanoparticles/nanorods array synthesized by thermal evaporation. *J. Alloys Compd.* **560**, 156–160 (2013)



16. Azarang, M., Shuhaimi, A., Yousefi, R., Jahromi, S.P.: One-pot sol–gel synthesis of reduced graphene oxide uniformly decorated zinc oxide nanoparticles in starch environment for highly efficient photodegradation of methylene blue. *RSC Adv.* **5**, 21888–21896 (2015)
17. Yousefi, R., Jamali-Sheini, F., Cheraghizade, M., Khosravi-Gandomani, S., SÁaedi, A., Huang, N.M., Basirun, W.J., Azarang, M.: Enhanced visible-light photocatalytic activity of strontium-doped zinc oxide nanoparticles. *Mater. Sci. Semicond. Process.* **32**, 152–159 (2015)
18. Zak, Khorsand: A., Majid, W.H.A., Darroudi, M., Yousefi, R.: Synthesis and characterization of ZnO nanoparticles prepared in gelatin media. *Mater. Lett.* **65**, 70–73 (2011)
19. Ghandomani, S., Yousefi, R., Jamli-Sheini, F., Ming Huang, N.: Optical and electrical properties of p-type Ag-doped ZnO nanowires. *Ceram. Int.* **40**, 7957–7963 (2014)
20. Azarang, M., Shuhaimi, A., Yousefi, R., Golsheikh, A.M., Sookhakian, M.: Synthesis and characterization of ZnO NPs/graphene oxide nanocomposite prepared in gelatin medium as highly efficient photo—degradation of MB. *Ceram. Int.* **40**(2014), 10217–10221 (2014)
21. Yousefi, R., Khorsand-Zak, A., Jamali-Sheini, F.: Growth, X-ray peak broadening studies, and optical properties of Mg-doped ZnO nanoparticles. *Mater. Sci. Semicond. Process.* **16**, 771–776 (2013)
22. Azarang, M., Shuhaimi, A., Yousefi, R., Sookhakian, M.: Effects of graphene oxide concentration on optical properties of ZnO/RGO nanocomposites and their application to photocurrent generation. *J. Appl. Phys.* **116**, 084307–084312 (2014)
23. Height, M.J., Pratsinis, S.E., Mekasuwandumrong, O., Prasertdam, P.: Ag-ZnO catalysts for UV-photodegradation of methylene blue. *Appl. Catal. B Environ.* **63**, 305–312 (2006)
24. Chen, C.C., Lu, C.S.: Mechanistic studies of the photocatalytic degradation of methyl green: an investigation of products of the decomposition processes. *Environ. Sci. Technol.* **41**, 4389–4396 (2007)
25. Kuo, T.J., Lin, C.N., Kuo, C.L., Hung, M.H.: Growth of ultralong ZnO nanowires on silicon substrates by vapor transport and their use as recyclable photocatalysts. *Chem. Mater.* **19**, 5143–5147 (2007)
26. Akyol, A.H., Yatmaz, C., Bayramoblu, M.: Photocatalytic decolorization of Remazol Red R in aqueous ZnO suspensions. *Appl. Catal. B Environ.* **54**, 19–24 (2004)
27. Monshi, A., Foroughi, M.R., Monshi, M.R.: Modified Scherrer equation to estimate more accurately nano-crystallite size using XRD. *World J. Nano Sci. Eng.* **2**, 154–160 (2012)
28. Baruah, S., Dutta, J.: Hydrothermal growth of ZnO nanostructures. *Sci. Technol. Adv. Mater.* **10**, 013001–013019 (2009)

